Absolute Radiation Measurement During Planetary Entry in the NASA Ames Electric Arc Shock Tube Facility

Brett A. Cruden[a]

[a]*ELORET Corporation, NASA Ames Research Center, MS 230-2, Moffett Field, CA 94035*

Abstract. During planetary entry, a shock-heated plasma that imparts significant heating to the structure is formed in front of the space vehicle. At high velocities, a significant portion of that energy transfer originates from radiation from the shock-heated plasma. Shock tubes are capable of simulating the high velocity and low density conditions typical of planetary entry and thus are able to recreate the radiative environment encountered by spacecraft. The Electric Arc Shock Tube (EAST) at NASA Ames Research Center is one of the few shock tubes in the world that is capable of reaching the high velocities that are necessary to study more extreme entry conditions. The EAST is presently being utilized to simulate radiation in a variety of planetary atmospheres. It is presently the only facility in which radiation originating in the vacuum ultraviolet is being quantified. This paper briefly describes recent tests in the EAST facility relevant to Earth, Mars, and Venus entry conditions, and outlines the issues in relating ground test data to flight relevant condition via predictive radiation simulations.

Keywords: Radiation, Planetary Entry, Shock Tube
PACS: 52.25.Os, 52.35.Tc, 52.70.Kz, 44.40.+a, 47.40.Ki, 47.70.-n

INTRODUCTION

During planetary entry conditions, the dissipation of space vehicle kinetic energy results in the formation of a shock-heated plasma in front of the spacecraft. Protection of the vehicle payload from the heat energy and power of the plasma requires development of thermal protection systems (TPS). Selection and sizing of appropriate TPS materials is the primary focus of spacecraft design and development, as too-thick TPS systems mean reduced payload mass or increased launch cost, while too-thin TPS systems could result in destruction of the payloads and mission failure. Sizing of the TPS is driven by modeling of the entry thermal environments and TPS material response to the imposed environments. Models that form the basis of simulations tools must be validated by (and often calibrated to) experimental data. Flight data which accurately represents the entry environment are very limited and often expensive to obtain, requiring ground tests to be performed which mimic the expected flight environments. Since it is generally not possible to entirely reproduce the characteristics of the entry plasma in ground facilities, plasmas which meet a certain subset of the condition are generated and studied, and models must be combined and/or extrapolated to predict performance. The TPS response requires a number of different ground tests in order to build comprehensive models. One component of this is the radiation produced in the plasma which may be absorbed by and converted to heat load (i.e., time-integrated heat flux) by the TPS. The overall importance of radiation in the heat load depends upon the size and trajectory of the spacecraft. Large vehicles or vehicles with high entry velocities will encounter greater heat load as the radiation magnitude scales as $\rho r v^8$ (in optically thick approximation). Examples of cases with large radiative heating include the Galileo probe to Jupiter, high mass (e.g. manned) Mars missions, Venusian entry and Lunar-return conditions for Orion/Apollo.

The radiation environment in this type of entry is simulated in shock tubes. In the shock tube, a pressure discontinuity which travels as a wave through a gas/gas mixture chosen to simulate the planetary atmosphere condition (composition and altitude/pressure) is introduced. Pressure discontinuities are generally induced by rupturing a diaphragm between high and low pressure regions. Methods of rupturing the diaphragm and creating the high pressure condition may involve pistons, heated gas, combustion or electric arcs. The Electric Arc Shock Tube (EAST) at NASA Ames, originally built in the 1960's is now the only shock tube of its type in operation. The

EAST facility schematic is shown in Fig. 1. The EAST is distinguished from other shock tubes presently in operation by its ability to obtain very high speed shock waves (up to 46 km/s). Recent tests have included Air re-entry for lunar return conditions[1,2] and Mars[3,4] and Venus[4] entry conditions for high mass landers and probes. Peak radiation for lunar return occurs at velocities between 9-11 km/s and pressures from 0.1-1.0 Torr, while the Mars and Venus conditions are primarily CO_2 gas, with 3.5-4% N_2, spanning 3-12 km/s and 0.01-2.0 Torr. Test campaigns so far have obtained comprehensive surveys and a number of high resolution images across a number of these conditions. This paper will briefly highlight the results obtained throughout these tests.

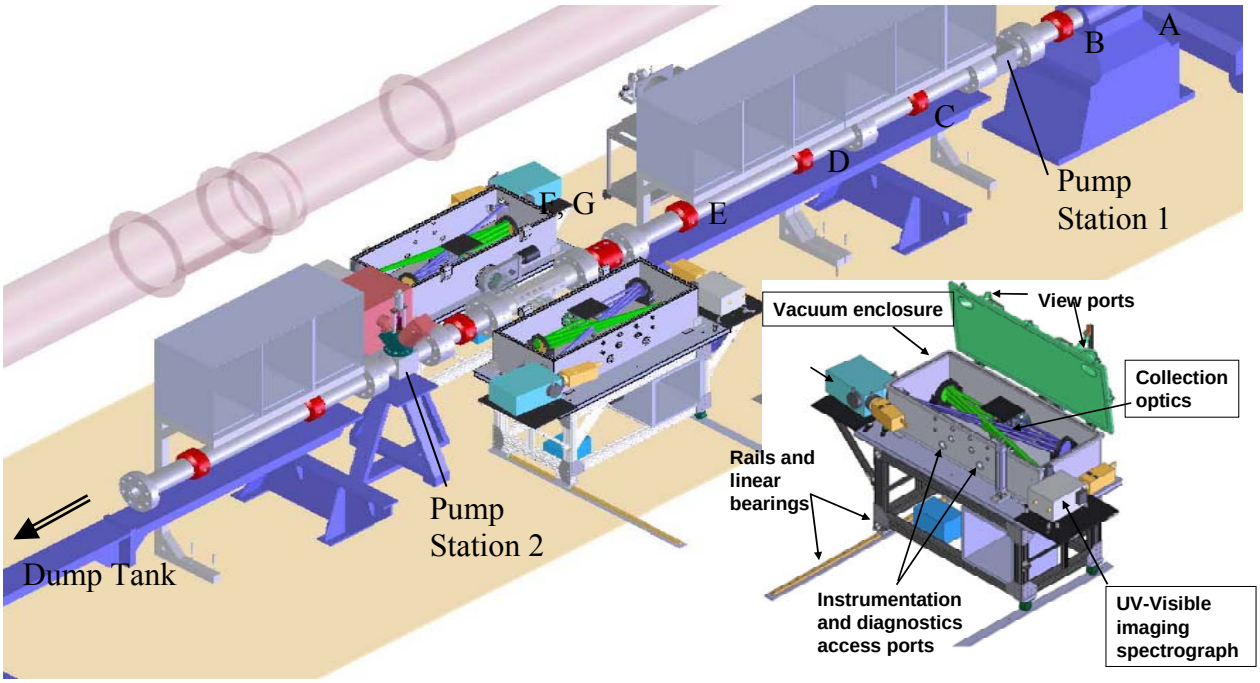

FIGURE 1. Schematic of the EAST facility. Inset shows the spectroscopic arrangement for vacuum ultraviolet imaging.

EXPERIMENTAL

High shock speeds are obtained in the EAST by using a high energy arc source in the driver section. A 1.3 mF capacitor bank capable of storing up to 1.2 MJ of energy is discharged into a helium gas volume of 1.3 L at up to 40 kV and >1 MA of current. This large amount of energy is dissipated over ~100 microseconds, resulting in a high energy pulse which drives a shock down the tube. The gas in advance of the driver is compressed, dissociated and ionized, simulating the conditions behind the bow shock around the vehicle during re-entry. While the separation between the driven and driver gas and the energy and composition in the driven gas does not make these conditions particularly useful for testing TPS materials, it is the only method available to produce the radiation spectrum expected under these conditions.

A pair of rectangular windows placed 180 degrees apart in the test section approximately 7.9 m downstream from the driver is used to collect radiance from the shock as it passes through. Four sets of collection optics focus the image of the windows onto one of four spectrometers, each tuned to a different wavelength range. CCDs connected to the spectrometer are triggered by a separate PMT, obtaining images of the shock wave in the same axial location of the tube. The imaging nature of the optics and spectrometer, along with the two dimensional CCD, allow for measurement of the radiance dependence on position in the shock tube along with the spectral resolution afforded by the dispersing nature of the spectrometer. The spectrometers are set to cover different spectral ranges from 120-1650 nm, such that it is now possible to obtain survey spectra covering this whole region in only two shots. Each spectrometer has high resolution capabilities, making it possible to measure individual atomic line broadening or to obtain molecular band structure in up to 4 regions simultaneously. Of particular interest for radiative heating is characterization in the vacuum ultraviolet (VUV), made important by the large radiance from low lying states of N and O atoms (in air) of the CO 4th positive sysem (in CO_2). The radiance in this region alone

has been predicted to account for half of the overall radiation but is made difficult to measure by the need to enclose the entire optical path in vacuum. To achieve this, the optics are entirely contained within large Al vacuum boxes, and the boxes are made to seal directly against the tube, with only the rectangular window separating the shock from the imaging system. Standard UV-grade fused silica windows are capable of obtaining spectral data down to ~160 nm. Further imaging down to 120 nm is made possible by the use of LiF window materials.

A sample spectrum obtained is shown in Fig. 2. This shows a 2-dimensional map of radiance as a function of position in the shock tube and wavelength as resolved by the spectrometer. Cross-sections in the vertical and horizontal direction show the absolute radiance versus these two parameters. The vertical cross section shows spectrally integrated radiance and identifies the major features of the shock wave. The presence of the shock front is detected at approximately 2 cm into the image by the large spike in radiance due to non-equilibrium radiation. This radiance quickly settles into a steady, position-independent radiance level that is typically assumed to be equilibrium radiation based on computational fluid dynamics (CFD) predictions. A second increase in radiation is observed at 10 cm, accompanied by the appearance of new spectral features. This marks the contact front, where the driver gas, with its contaminants such as Al, W and CF_2, produces new radiation features. The valid test region is that between the shock and contact front, with the majority of this work focusing on the radiation features in the "equilibrium" zone.

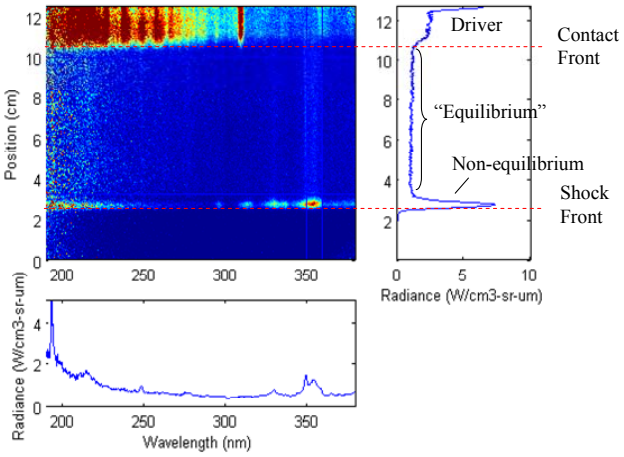

FIGURE 2. Sample 2d data obtained and interpretation for a typical lunar return air shock.

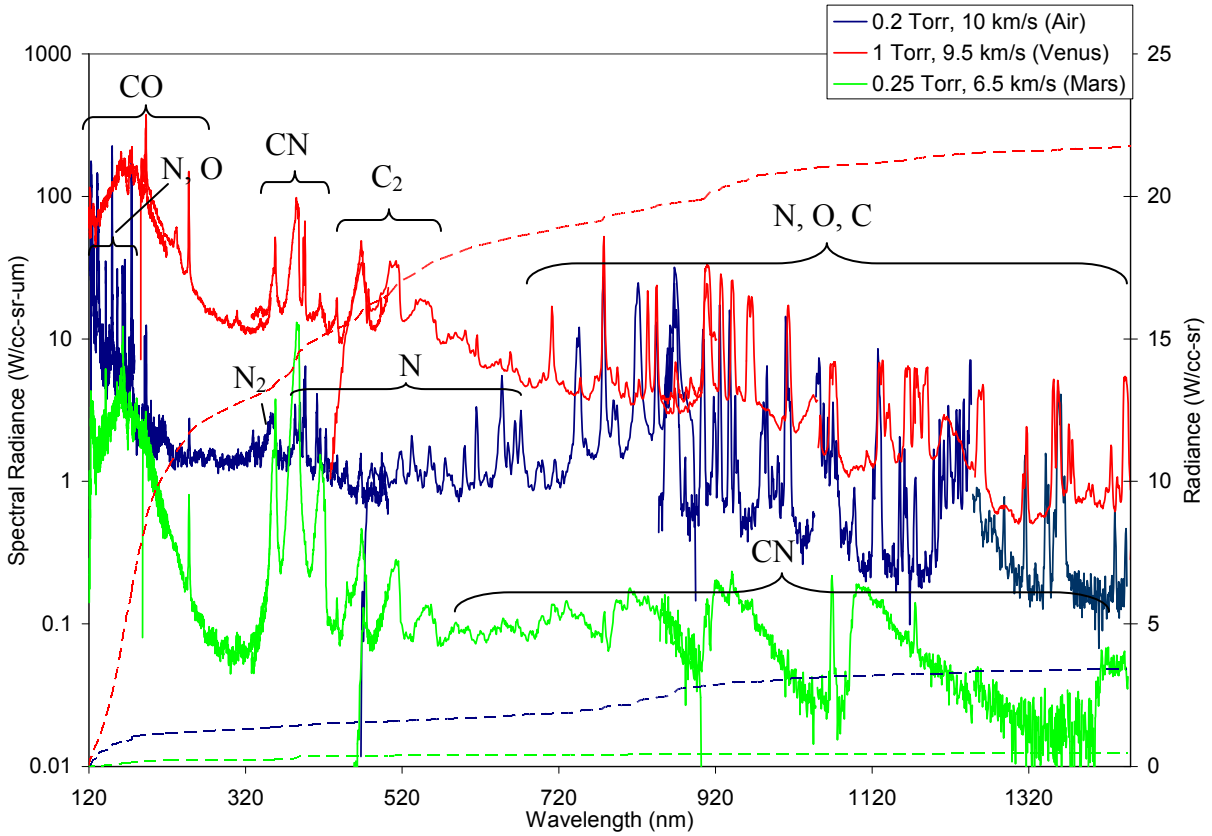

FIGURE 3. Composite spectra obtained in three different planetary entry conditions.

RESULTS

Fig. 3 shows a composite image of radiation spectra obtained in the "equilibrium" region for some representative conditions in each of the 3 atmospheres studied. The plots are shown on log scale so that all features may be seen in the same figure. The relatively lower entry velocities for Mars entry make it a more benign radiation condition, while Venus, with its high atmospheric density and large entry velocities, presents a much higher radiative magnitude. Earth entry for lunar return is between the two cases in magnitude. All three spectra are characterized by a broad continuum baseline emission and by different atomic features. The continuum is usually attributed to collision processes involving free electrons. Bremsstrahlung is one such process but at the densities and temperatures encountered for entry conditions, free-bound processes such as radiative attachment and recombination are more likely to be the continuum radiation sources. However, the best cross-sections presently available for predicting the continuum magnitude substantially underpredict the observed radiation under equilibrium assumption. The spectral features of the shock are dependent upon the gas being tested and the velocity condition. Mars and Venus entry show some similar features including CO 4^{th} positive radiation below ~200 nm, CN Violet radiation between 320-450 nm and C_2 Swan bands from 450-600 nm. At low velocity, the CN red system is apparent and extends through the Near-IR. At higher velocity, atomic radiation features from C and O atoms become prominent in the Near-IR. Above 10 km/s (not shown here), molecular dissociation results in near-elimination of CO, CN and C_2 radiation and the appearance of many atomic lines across the entire wavelength range. The air entry condition of 10 km/s shown in Fig. 3 also shows near-complete dissociation and significant atomic line radiation from N and O atoms. At lower velocity, air may show some molecular features from N_2, N_2^+ and NO. The integral of the spectral radiance, or radiance (dashed lines), shows that approximately half of the total radiation is contributed from vacuum ultraviolet features in all three of these cases.

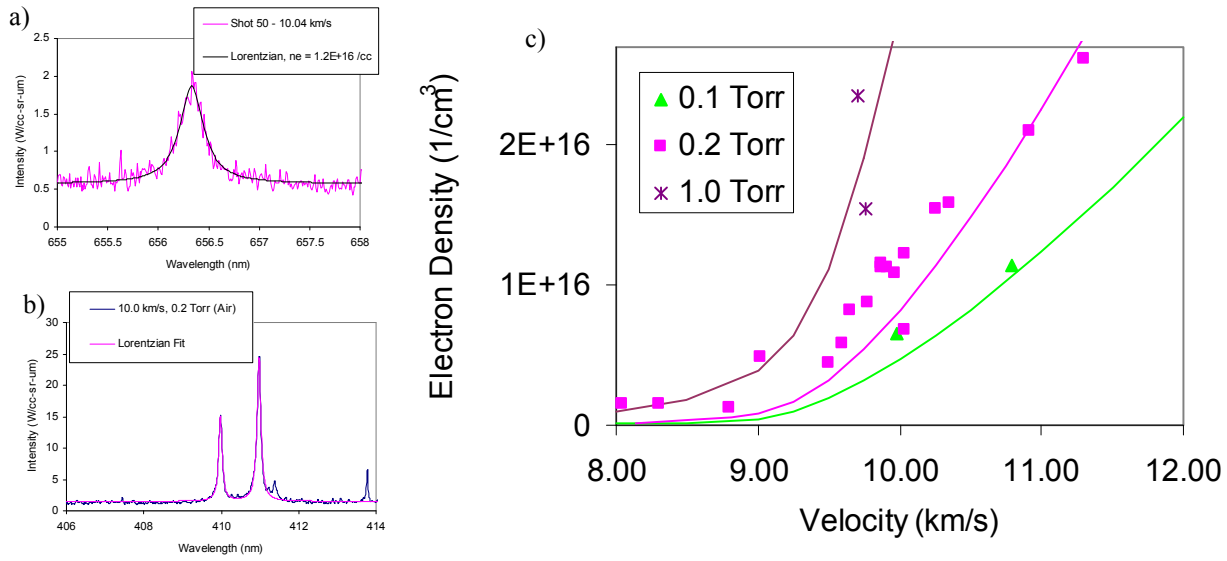

FIGURE 4. Stark broadening measurement in air shocks. (a) Shows the Hα line with corresponding Lorentzian line fit. (b) Lorentzian line fit of N 409.99 and 410.99 nm lines. (c) Summary of electron density measurement versus velocity in air at three pressures. Solid lines depict equilibrium condition while points are the experimentally measured data.

The presence of the larger than expected background continuum has led us to reconsider some of the assumptions inherent in the method of analysis. One such assumption is that shock-heated gas mixture relaxes to thermodynamic equilibrium (as given by Rankine-Hugoniot relations for an equilibrium gas mixture) behind the shock front. Application of Rankine-Hugoniot relations for a normal shock with appropriate input thermochemical data results in unique temperature, pressure and mole fractions obtained behind the shock. The electron number density behind the shock wave may therefore be measured to test the equilibrium assumption. Stark broadening of several lines has thus been used to determine the electron number density.[1] The majority of atomic lines present under most conditions do not have measurable broadenings with the use of 0.5m grating spectrometers. A notable exception is Hydrogen which was present as an impurity in the shock tube. The width of both Hydrogen Balmer α

and β lines has been measured over many of the conditions studied for air shocks and in general agreed with each other to within 10%. Experiments were also performed with varying degrees of Hydrogen loading, and the result was found to be independent of the Hydrogen mole fraction up to 2%. At 10 km/s and 0.2 Torr pre-shock pressure, the electron number density was measured to be between 1.2-1.8 x 10^{16} cm^{-3} (Fig 4(a)). This result was later checked against the broadening of some weaker N lines near 410 nm (Fig. 4(b)) and O at 533 nm (not shown), which gave consistent number density results of 1.4-1.6 x 10^{16} cm^{-3}. This solution is approximately a factor of two larger than the equilibrium solution of 8.2 x 10^{15} cm^{-3}. The reason for this discrepancy is not yet completely understood. Fig. 4(c) below shows the summary of electron number density measurement over a range of velocities and pressures as measured by the Stark broadening of the atomic Hydrogen lines, Hα and Hβ. The solid lines represent the equilibrium solution. It is apparent that disagreement between theory and measurement is observed over most conditions, becoming worse at low velocities, and better at the highest velocities studied experimentally. The discrepancy would be equivalent to a 3% shift in velocity if factors such as shock deceleration or velocity measurement accuracy were to be considered. (Error in velocity measurement is between 0.5-1.5%, though due to deceleration and compression, a portion of the gas measured was initially shocked at a velocity that is about 3% higher). Alternatively, a deviation in temperature of 500-1000K from equilibrium would be required to match the measured electron densities.

Under similar conditions of pure N_2, a similar magnitude of continuum radiation has been observed in electric arc shock tubes as far back as 1964.[5,6] At the time, the mechanism for the radiation was attributed to radiative attachment of the N atom, i.e. $N + e^- \rightarrow N^-$. However, this proposed mechanism has more recently been rejected by the community as better computational tools revealed the low stability of the N cation. More recent computations of radiation by this mechanism has suggested it may be a significant contributor to radiation[7] although the suggested cross-sections for this reaction do not provide the correct spectral dependence or magnitude, as shown in Fig 5. However, recent recomputation of the radiative recombination with the nitrogen anion shows a similar spectral dependence to the experimental observation.[8] Based on equilibrium electron densities, the nitrogen radiation would still be too small. However, if the experimentally measured electron density is used instead, the continuum magnitude now comes into agreement with the observation. The magnitude of this radiation is quite sensitive to the electron density, since quasineutrality results in the recombination rate, and hence radiation magnitude, scaling as n_e^2. If the shock wave temperature or velocity were elevated to match this continuum at equilibrium, the predicted atomic line radiation would correspondingly increase. Therefore, the radiation spectrum appears to indicate that the electronic population of the neutral atoms has attained an equilibrium profile, while the ionization fraction is not. How this could be possible is unclear. While the case of the background continuum radiation in Mars and Venus entry has not yet been explored in as great detail, it is expected that similar mechanisms may exist to explain the discrepancy.

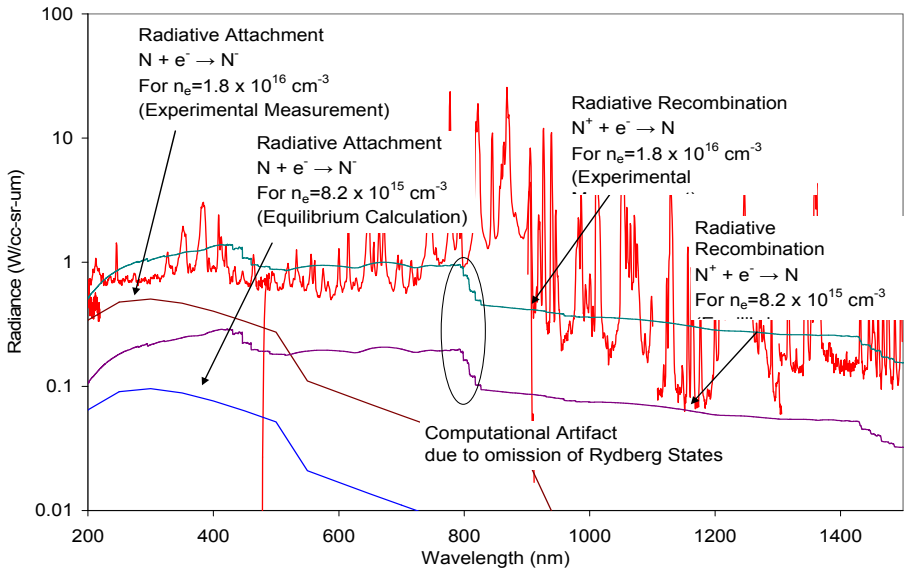

FIGURE 5. Possible mechanisms for background continuum. Overlaid on measured experimental data are the predicted contributions from two continuum emission process, using two different electron densities. It is found that radiative attachment is too small and displays the wrong shape to match experiment, while the radiative recombination is consistent with experimental data if the experimentally measured electron density is used instead of the equilibrium electron density.

CONCLUSIONS

The NASA Ames EAST facility is a unique facility capable of measuring radiative environments relevant to planetary entry over a wide range of conditions. Of particular note is the capability of measuring absolute radiance over the range of 120-1650 nm for a single condition. Four spectra collect data simultaneously, such that the entire range can be monitored, with spatial resolution, in only two tests. High resolution capabilities exist throughout this range, allowing for spectral features to be monitored for broadening and temperature. Some representative data is presented for Mars, Venus and Earth entry condition. Of particular concern from the measured data is a background continuum that is substantially larger than that predicted under equilibrium radiation. Stark broadening of Hydrogen, Nitrogen and Oxygen lines has been used here to quantify electron density in the shock, and it is found that the electron density exceeds equilibrium for most conditions, contrary to the predictions of CFD tools on comparable blunt bodies. This elevated electron density may explain much of the discrepancy in background continuum, however the reason for this difference, and the impact it may have in flight condition relative to the ground test is a challenge that remains to be understood.

ACKNOWLEDGMENTS

The author would like to acknowledge Mark McGlaughlin and James Joyce for facility operation, Ramon Martinez and Hai Le for data collection and Drs. Jay Grinstead, Deepak Bose, David Bogdanoff, Dinesh Prabhu, Michael Winter, Aaron Brandis, Duane Carbon and Winifred Huo for useful discussion throughout the course of this work. Support for Air Testing is provided by CEV Aeroscience Program (Dr. Joseph Olejniczek, Program Manager), Mars Testing from NASA Fundamental Aeronautics Program, Hypersonics Project – Aerodynamics, Aerothermodaynamics and Plasmadynamics (AAP) Discipline (Dr. Deepak Bose, Associate Principal Investigator) and Venus Tests from by the In-Space Propulsion Program under task agreement M-ISP-08-13 to NASA Ames (Dr. Michael Wright, Co-Investigator). The author has been supported on this work on NASA Contract NNA04BC25C to ELORET.

REFERENCES

1. Brett A. Cruden, Ramon Martinez, Jay H. Grinstead et al., 41st AIAA Thermophysics Conference Proceedings, AIAA, San Antonio, TX, 2009, AIAA 2009-4240.
2. Jay H. Grinstead, Michael C. Wilder, Joseph Olejniczak et al., 46th AIAA Aerospace Sciences Meeting Proceedings, AIAA, Reno, Nevada, 2008, AIAA 2008-1244.
3. Jay H. Grinstead, Michael C. Wilder, Michael J. Wright et al., 46th AIAA Aerospace Sciences Meeting Proceedings, AIAA, Reno, Nevada, 2008, AIAA 2008-1272.
4. Brett A. Cruden, Dinesh Prabhu, Ramon Martinez et al., 10th AIAA/ASME Joint Thermophysics and Heat Transfer Conference Proceedings, AIAA, Chicago, IL, 2010, AIAA-2010-4508.
5. D. L. Ciffone and J. G. Borucki, *Journal of Quantitative Spectroscopy and Radiative Transfer* **11**, 1291-1310 (1971).
6. R. A. Allen and A. Textoris, *The Journal of Chemical Physics* **40**, 3445 (1964).
7. C. O. Johnston, B. R. Hollis, and K. Sutton, *Journal of Spacecraft and Rockets* **45**, 865–878 (2008).
8. W. M. Huo, 46th AIAA Aerospace Sciences Meeting Proceedings, AIAA, Reno, NV, 2008, AIAA 2008-1207.